Analysis increase in the efficiency of a-Si: H solar cell due to the addition of an intrinsic layer to the p-i-n structure by ellipsometric spectroscopy

SONI PRAYOGI (prayogi.sp@gmail.com)
Universitas Syiah Kuala https://orcid.org/0000-0002-2996-5047
Yoyok Cahyono
Institut Teknologi Sepuluh Nopember
Darminto D
Institut Teknologi Sepuluh Nopember

Research Article

Keywords: Solar cell, a-Si: H, p-i-n, p-i1-i2-n, PECVD, ES

DOI: https://doi.org/10.21203/rs.3.rs-188559/v1

Abstract

Backround:

In this study, we report for the first time that the addition of an intrinsic layer to the a-Si: H p-i-n solar cell structure greatly enhances the conversion efficiency. The a-Si: H p-i-n solar cells were grown using *Plasma Enhanced Chemical Vapor Deposition* (PECVD) techniques on the *Indium Tin Oxide* (ITO) substrate and added an intrinsic layer with the p-i_1-i_2-n structure in order to prevent sunlight energy from being absorbed the first intrinsic layer can be absorbed by the second intrinsic layer.

Result

The a-Si: H p-i-n and p-i_1-i_2-n solar cells were characterized including optical properties, electrical properties, surface morphology, thickness, band-gap using *Ellipsometric Spectroscopy* (ES). Furthermore, from the optical constant and thin film thickness, the reflectance and transmittance of each sample were obtained. The p-i-n and p-i_1-i_2-n samples show good transparency in the infrared region and this transparency decreases in the visible light region shows an interference pattern with a sharp decrease in transmission at the absorption edge and the performance of solar cells (curve I-V) measured by use sun simulator and sunshine.

Conclussion:

Our results show that there is a very good increase in the efficiency of the a-Si: H p-i_1-i_2-n solar cells by 58.6% of the original p-i-n structure.

1. Background

One of the main problems found in hydrogenated amorphous silicon (a-Si: H) based solar cells is the instability of their efficiency after being exposed to high intensity for a long period of time. This phenomenon is known as the *Staebler-Wronski Effect* (SWE)(Panchal et al., 2011). The high hydrogen content is then known as one of the causes of SWE, where the silicon-hydrogen bond is easily released by the influence of high-intensity irradiation, leaving defects in the solar cell material(Nguyen et al., 2016). Therefore, several researchers then developed the *Plasma Enhanced Chemical Vapor Deposition* (PECVD) technique to overcome this problem. Material a-Si: H grown with PECVD by utilizing plasma as a growing medium(Bougoffa et al., 2017). This technique uses Silan gas (SiH_4) as the source gas, which is 10% in Hydrogen (H_2) gas and an amorphous silicon material with a hydrogen content of 10–20% is obtained(King et al., 2011).

Increasing the efficiency of hydrogenated amorphous silicon (a-Si: H) based solar cells, especially to optimize the quality of the thin film on the p-i-n part of the solar cell, this part is the main part to convert

solar energy into electrical energy(Fantoni et al., 2018). If the quality in the manufacture of this thin layer of p-i-n solar cells is good, the efficiency of solar cells can increase between 5–21%(Schulze et al., 2012). Meanwhile, the concentration of boron or phosphorus dopants can affect the type of thin layer formed, so that the electron and hole concentrations can be controlled(Muhammad et al., 2015). Usually the energy gap width in p-i-n solar cells also greatly affects the magnitude of the conversion efficiency of solar cells, it is also required to have a high absorption rate so that the photovoltaic effect obtained can be optimum(Rolland et al., 2017).

In this study, we reported the characteristics of hydrogenated amorphous silicon (a-Si: H) based solar cells with the addition of an active layer (i-layer) using ellipsometric spectroscopy (ES). As we know, the i-layer of the a-Si: H-based p-i-n solar cell device plays the most important role in the utilization of photon energy to excite its charge carrier from the valence band to the conduction band(Levallois et al., 2006). On the one hand, more photons will be absorbed if the active layer is thicker so that the charge carrier generation rate increases. On the other hand, the thicker i-layer also contributes to an increase in the localized state as well as an increase in the series resistance, thereby reducing the conversion efficiency of the solar cell(Aliani et al., 2018). Therefore, the addition of the active layer (i-layer) with the optimum thickness will provide the best characteristics directly by maintaining the quality of the material, which is indirectly related to the technique used when growing the material.

2. Methods

In the research conducted, solar cells a-Si: H were grown on a *Corning 7059 glass* substrate coated with *Indium Tin Oxide* (ITO). The PECVD engineering system used consists of a multi chamber with two deposition chambers, each of which is used specifically to deposit the intrinsic layer and the extrinsic layer as shown in Figure 1.The filament tension used is still off (0 volts) to ensure that the resulting layer is still amorphous in structure(Cahyono et al., 2018). In this condition, the filament temperature is only determined by the radiation heater temperature (*substrate temperature*). Silane gas (SiH_4) with a concentration of 10% in hydrogen (H2) is used as the source gas(Prayogi et al., 2017). As dopant gas, B_2H_6 gas with 10% concentration in H_2 for dopant p-type layers was used and PH_3 gas with 10% concentration in H_2 for n-type layer dopants(Prayogi et al., 2019). The growth parameters used are as shown in Table-1 and Table 2.

[Fig. 1 about here.]

[Table. 1 about here.]

[Table. 2 about here.]

The optimization of the thickness of the active layer is carried out based on the recommendations of the simulation results regarding the thickness range that can produce

solar cells with good characteristics. Therefore, the thickness of the i-layer was varied between 4400-6000 Å, while the thickness of the p-layer and the n-layer was maintained at 150 Å and 300 Å, respectively(Franta et al., 2013). In this research, a-Si: H solar cell is fabricated by joining the p-i-n and p-i_1-i_2-n structures schematically as shown in Figure 2.

[Fig. 2 about here.]

Ellipsometric spectroscopy (ES) was used in this research to obtain the transmittance data and mechanisms which broaden or shift the exciton resonance such as impurities, doping, strain, and phonon interactions, in turn, broaden and shift the absorption band edge and influence the optical constants near the band gap(Yousif et al., 2019). All measurements were done at 70° incidence with a spot size of approximately 2 mm. Measurements with UVISEL were done over the range 0.6 eV to 6.5 eV (~ 2060 - 190 nm). In this paper, the results of transmission measurements which are used to determine the absolute value of the absorption coefficient will be reported. Powerful DeltaPsi2 software from research to routine. The DeltaPsi2 software platform provides complete functionality for measurements, modeling, and reporting in addition to automatic operations, which facilitate routine thin film analysis(Oates et al., 2011). The multitasking software provides the ultimate in versatility for use in ex-situ and in-situ configurations as well as the ability to drive the large range of accessories available(Dahal et al., 2014). The DeltaPsi2's intuitive operation meets the requirements of both experienced SE scientists and newcomers to the technique.

To determine the performance of the resulting solar cells, the current-voltage (I-V) characteristics of the solar cells are measured under irradiation with a fixed intensity. In this study, I-V characteristics were measured using a *Keithley 617*. As a light source, halogen lamps were used at an intensity of 34 mW/cm^2. From the measurement of the I-V characteristics, the parameters of solar cells include open-circuit voltage (V_{OC}), short-circuit current (I_{SC}), maximum operating point for determining the fill factor (FF), and conversion efficiency (η)(Seba et al., 2020). At the maximum operating point, the maximum voltage (V_m) and maximum current (I_m) are known(Kumar Saha et al., 2010). Conversion efficiency is the ratio between the output power of the solar cell (P_{out}) to the power supplied (P_{in}), determined by relationship:

$$\eta = \frac{P_{out}}{P_{in}} = \frac{FF.V_{oc}.I_{sc}}{\Phi A} x\ 100\% \quad (1)$$

where Φ is the irradiation intensity and A is the area of the solar cell. Whereas FF is determined by relationship:

$$FF = \frac{I_m V_m}{I_{sc} V_{oc}} \quad (2)$$

3. Results

The ψ and **Δ** experiments for p-i-n, p-i_1-i_2-n and Indium Tin Oxide (ITO) substrates are shown in Fig. 3 together with the fittings of the analysis. To support the optical and electronic analysis of the respective material in the graph plot the real part < ε_1 > and < ε_2 > imaginary part of the complex dielectric function is derived using spectroscopic ellipsometric data for three pin samples, p-i_1-i_2-n and Indium Tin Oxide (ITO) substrate. Measured at room temperature in the optical energy range 0.6–6.6 eV.

[Fig. 3 about here.]

The results of measurements and fittings of p-i-n, p-i_1-i_2-n and ITO substrates obtained information and parameters from the optical properties of the material, including refractive index, dielectric constant, absorption coefficient, and thickness. Furthermore, from the optical constant and thin film thickness, the reflectance and transmittance of each sample were obtained. In the p-i-n sample, p-i_1-i_2-n shows good transparency in the infrared region and this transparency decreases in the visible region. The spectrum shows an interference pattern with a sharp decrease in transmission at the absorption edge.

[Fig. 4 about here.]

The result of Fig. 4 dielectric function (ε) describes the optical and electrical properties of the material over the measurement energy range. The dielectric function consists of two components, namely real (ε_1) and imaginary (ε_2). The real component ε_1 represents the polarization of the material due to the electric dipole which contributes to the atomic and electric polarization, while the imaginary component ε_2 represents the amount of light absorption in the material(Kanneboina et al., 2018). The real component ε_1 shows the value of E_0 in the p-i-n sample of 2.86 eV and the sample p-i_1-i_2-n of 2.66 eV. Where there is a change in the E_0 energy in the p-i_1-i_2-n sample which changes the energy to a smaller one compared to the pin sample with a large change of 0.20 eV, this proves that at that energy the p-i_1-i_2-n sample can absorb more energy. larger than the sample pin and ultimately can improve the performance of these solar cells. Whereas in the imaginary component ε_2, the value of E_1 in the p-i-n sample and the p-i_1-i_2-n sample does not change.

The value of the complex refractive index (*n* and *k*) obtained by measuring ellipsometric spectroscopy describes the value of *n* which represents the refractive index of the material and the value of *k* which represents the extinction coefficient of absorption of material and energy lost due to the scattering process(Chakraborty et al., 2014). Figure 5 shows the optical properties of the p-i-n sample layer and the p-i_1-i_2-n sample layer for measurement at the same temperature over the ITO substrate. In the p-i_1-i_2-n sample, the a-Si: H film quality was obtained which was quite good in terms of the lowest n value compared to the p-i-n sample. At energy < 3.0 eV in *n* samples p-i_1-i_2-n there is a decrease compared to pin samples, this illustrates that the maximum absorption rate obtained is greater for samples p-i_1-i_2-n than for pin samples even though for each sample it is measured at the same substrate temperature. During deposition the substrate temperature greatly affects the diffusion process of the pinned target atoms deposited on the substrate. In this case because the substrate temperature will cause the atoms of the substrate surface to vibrate and as a consequence the distance between the planes stretches, thus facilitating the process of insertion (interstition)(Boosalis et al., 2011). Furthermore, seen from the *k* value in the p-i_1-i_2-n sample, it is found that > 3.0 eV is a greater value than in the p-i-n sample, this indicates that the results of the p-i_1-i_2-n sample are denser than the p-i-n sample. However, at energy < 1.8 eV, a thin, more transparent layer is produced, as evidenced by the negative value of *k*, this is likely to occur saturation of the insertion process of the twisted atoms and consequently a layer that is not dense/porous(Kim et al., 2012).

[Fig. 5 about here.]

4. Discussion

The characterization of the pin sample solar cells and the p-i_1-i_2-n sample were measured using *Keithley 617*. Figure 6 shows the results of the measurement results of the I-V characteristics of solar cells a-Si: H produced in the pin sample and p-i_1-i_2-n sample with an increase in efficiency of 58.6%. Overall, the a-Si: H solar cells produced still have a low fill factor value, indicated by the low maximum output power. One of the factors that caused the low fill factor value of the solar cell samples p-i-n and the resulting p-i_1-i_2-n samples was the imperfect joint formation mechanism that created defect conditions in the interface area. It is known that the p-i-n sample solar cell produced has four junction regions, and the p-i_1-i_2-n sample solar cell produced has five junction regions. Each of these is a connection between the ITO-layer and the p-layer, between the p-layer and the i_1-layer, between the i-layer and the i_2-layer, between the i_2-layer and the n-layer, and between the n-layer and metal contacts. If the connection between these layers is not formed properly it will create defect conditions in the joint area. The defects formed in each junction will also make a major contribution to the increase in the value of the series resistance of the solar cell samples p-i-n and samples p-i_1-i_2-n. If this happens, the current generated by the irradiation effect (*photo current*) will decrease rapidly with increasing bias voltage(Kunc et al., 2019). Even so, all of the p-i-n sample solar cells and the p-i_1-i_2-n samples produced had a fairly good internal charging of the electric field, indicated by a fairly high V_{OC} value(Filali et al., 2016).

[Fig. 6 about here.]

As explained above, the solar cell device layer of the pin sample and sample p-i_1-i_2-n plays the most important role in the utilization of photon energy to excite its charge carrier from the valence band to the conduction band and the electric field strength formed between the p-layer. and layer-n. More photons will be absorbed if the active layer is thicker so that the charge carrier generation rate increases(Funke et al., 2017). However, the thicker i-layer also contributes to the increase in series resistance (R_s) due to the localized conditions which will also increase. On the other hand, an i-layer that is too thin will cause a weakening of the electric field formed between the p-layer and the n-layer(Laatar et al., 2017). Apart from series resistance, another factor that influences the characteristics of the solar cell samples p-i-n and samples p-i_1-i_2-n is the shear resistance value (R_{sh}). This resistance is related to the process of charge carrier recombination from the conduction band to the valence band. In the p-i-n sample solar cell and p-i_1-i_2-n sample, recombination between the bands is not expected because it will decrease the electron flow (current flow) from the n-layer to the p-layer(Schamm-Chardon et al., 2011). However, this phenomenon cannot be avoided in the pin sample solar cells and the p-i_1-i_2-n sample because the a-Si: H material has localized states in the energy bandgap region where this will increase the likelihood of recombination. between the ribbons. Therefore, the ideal solar cell has a very large R_{sh} value and a very small R_s value.

5. Conclusion

Based on the results obtained in this study, it was reported that the characteristics of solar cells based on hydrogenated amorphous silicon (a-Si: H) with the addition of an active layer (i-layer) using ellipsometry spectroscopy obtained a fairly good increase in conversion efficiency (58.6%). The conversion efficiency of solar cells produced by the addition of the active layer (i-layer) is still possible to improve, among others, such as insertion of a buffer layer in the areas between layers, the use of p-layer with doping-delta (δ-doped) which is proven to be able to improve the performance of a-Si: H solar cells with a uniform doping p-layer, the use of a-SiC: H material in the p-layer which is known to be more transparent than a-Si: H, or the use of a tandem structure (a-Si: H based pin solar cell for upper cells connected with p-i-n solar cells based on μc-Si: H for bottom cells).

Acknowledgement

One of the authors (SP) thankfully acknowledges the Ministry of Finance of the Republic of Indonesia, through the Lembaga Pengelolah Dana Pendidikan (LPDP), which has provided financial support through the Scholarship Indonesian. The authors would also appreciate LPPM Institut Teknologi Sepuluh Nopember for the use of experimental facilities at Research Center ITS and Dr. Michael Tchaikovsky, HORIBA Scientific, France. For measuring samples using UVSEL Ellipsometric Spectroscopy. We are thankful to Prof. Andrivo Rusydi who provided a fruitful discussion for this paper.

References

Aliani, C., Krichen, M., Zouari, A., 2018. Influence of the semiconductor/metal rear contact on the performance of n(a-Si:H)/i(a-Si:H)/p(c-Si) heterojunction solar cells. Opt. Quantum Electron. 50, 296.

Boosalis, A., Hofmann, T., Šik, J., Schubert, M., 2011. Free-charge carrier profile of iso- and aniso-type Si homojunctions determined by terahertz and mid-infrared ellipsometry. Thin Solid Films, 5th International Conference on Spectroscopic Ellipsometry (ICSE-V) 519, 2604–2607.

Bougoffa, A., Trabelsi, A., Zouari, A., Dhahri, E., 2017. A new modeling approach for amorphous silicon passivated front contact for thin silicon solar cells. Opt. Quantum Electron. 49, 259.

Cahyono, Y., Yahya, E., Zainuri, M., Pratapa, S., Darminto, 2018. Quantum Confinement in an Intrinsic a-Si:H Thin Film Deposited on Soda Lime Glass Substrate Using PECVD. Trans. Electr. Electron. Mater. 19, 69–73.

Chakraborty, M., Banerjee, A., Das, D., 2014. Spectroscopic studies on nanocrystalline silicon thin films prepared from H2-diluted SiH4-plasma in inductively coupled low pressure RF PECVD. Phys. E Low-Dimens. Syst. Nanostructures 61, 95–100.

Dahal, L.R., Li, J., Stoke, J.A., Huang, Z., Shan, A., Ferlauto, A.S., Wronski, C.R., Collins, R.W., Podraza, N.J., 2014. Applications of real-time and mapping spectroscopic ellipsometry for process development and optimization in hydrogenated silicon thin-film photovoltaics technology. Sol. Energy Mater. Sol. Cells, Thin film photovoltaic materials and device physics 129, 32–56.

Fantoni, A., Fernandes, M., Vygranenko, Y., Louro, P., Vieira, M., Silva, R.P.O., Texeira, D., Ribeiro, A.P.C., Prazeres, M., Alegria, E.C.B.A., 2018. Analysis of metallic nanoparticles embedded in thin film semiconductors for optoelectronic applications. Opt. Quantum Electron. 50, 246.

Filali, L., Brahmi, Y., Sib, J.D., Bouhekka, A., Benlakehal, D., Bouizem, Y., Kebab, A., Chahed, L., 2016. The effect of amorphous silicon surface hydrogenation on morphology, wettability and its implication on the adsorption of proteins. Appl. Surf. Sci. 384, 107–115.

Franta, D., Nečas, D., Zajíčková, L., Ohlídal, I., Stuchlík, J., 2013. Advanced modeling for optical characterization of amorphous hydrogenated silicon films. Thin Solid Films, Current Trends in Optical and X-Ray Metrology of Advanced Materials for Nanoscale Devices III 541, 12–16.

Funke, S., Wurstbauer, U., Miller, B., Matković, A., Green, A., Diebold, A., Röling, C., Thiesen, P.H., 2017. Spectroscopic imaging ellipsometry for automated search of flakes of mono- and n-layers of 2D-materials. Appl. Surf. Sci., 7th_International Conference on Spectroscopic Ellipsometry 421, 435–439.

Kanneboina, V., Madaka, R., Agarwal, P., 2018. Spectroscopic ellipsometry studies on microstructure evolution of a-Si:H to nc-Si:H films by H2 plasma exposure. Mater. Today Commun. 15, 18–29.

Kim, S., Dao, V.A., Shin, C., Cho, J., Lee, Y., Balaji, N., Ahn, S., Kim, Y., Yi, J., 2012. Low defect interface study of intrinsic layer for c-Si surface passivation in a-Si:H/c-Si heterojunction solar cells. Thin Solid Films,

The 3rd International Conference on Microelectronics and Plasma Technology (ICMAP) 2011 521, 45–49.

King, S.W., Bielefeld, J., French, M., Lanford, W.A., 2011. Mass and bond density measurements for PECVD a-SiCx:H thin films using Fourier transform-infrared spectroscopy. J. Non-Cryst. Solids 357, 3602–3615.

Kumar Saha, J., Ohse, N., Hamada, K., Matsui, H., Kobayashi, T., Jia, H., Shirai, H., 2010. Fast deposition of microcrystalline Si films from SiH2Cl2 using a high-density microwave plasma source for Si thin-film solar cells. Sol. Energy Mater. Sol. Cells 94, 524–530.

Kunc, J., Rejhon, M., Dědič, V., Bábor, P., 2019. Thickness of sublimation grown SiC layers measured by scanning Raman spectroscopy. J. Alloys Compd. 789, 607–612.

Laatar, F., Harizi, A., Ghrib, M., Hassen, M., Khirouni, K., Gaidi, M., Ezzaouia, H., 2017. Rapid thermal annealing effect on the microstructural and optical properties of nc-Si embedded in porous anodic alumina. J. Alloys Compd. 709, 487–495.

Levallois, C., Le Corre, A., Dehaese, O., Folliot, H., Paranthoen, C., Labbé, C., Loualiche, S., 2006. Design and Fabrication of GaInAsP/InP VCSEL with Two a-Si/a-SiNxBragg Reflectors. Opt. Quantum Electron. 38, 281–291.

Muhammad, M.H., Hameed, M.F.O., Obayya, S.S.A., 2015. Broadband absorption enhancement in periodic structure plasmonic solar cell. Opt. Quantum Electron. 47, 1487–1494.

Nguyen, H.T., Rougieux, F.E., Yan, D., Wan, Y., Mokkapati, S., de Nicolas, S.M., Seif, J.P., De Wolf, S., Macdonald, D., 2016. Characterizing amorphous silicon, silicon nitride, and diffused layers in crystalline siliconsolarcellsusingmicro-photoluminescence spectroscopy. Sol. Energy Mater. Sol. Cells 145, 403–411.

Oates, T.W.H., Wormeester, H., Arwin, H., 2011. Characterization of plasmonic effects in thin films and metamaterials using spectroscopic ellipsometry. Prog. Surf. Sci. 86, 328–376.

Panchal, A.K., Rai, D.K., Mathew, M., Solanki, C.S., 2011. a-Si/SiNxmultilayered light absorber for solar cell. J. Nanoparticle Res. 13, 2469–2473.

Prayogi, S., Ayunis, Kresna, Cahyono, Y., Akidah, Darminto, 2017. Analysis of thin layer optical properties of A-Si:H P-Type doping CH4 and P-Type without CH4 is deposited PECVD systems 853, 012032.

Prayogi, S., Baqiya, M.A., Cahyono, Y., Darminto, 2019. Optical Transmission of p-Type a-Si:H Thin Film Deposited by PECVD on ITO-Coated Glass [WWW Document]. Mater. Sci. Forum. URL https://www.scientific.net/MSF.966.72 (accessed 11.23.20).

Rolland, A., Pedesseau, L., Kepenekian, M., Katan, C., Huang, Y., Wang, S., Cornet, C., Durand, O., Even, J., 2017. Computational analysis of hybrid perovskite on silicon 2-T tandem solar cells based on a Si tunnel junction. Opt. Quantum Electron. 50, 21.

Schamm-Chardon, S., Coulon, P.E., Lamagna, L., Wiemer, C., Baldovino, S., Fanciulli, M., 2011. Combining HRTEM–EELS nano-analysis with capacitance–voltage measurements to evaluate high-κ thin films deposited on Si and Ge as candidate for future gate dielectrics. Microelectron. Eng., Post-Si-CMOS electronic devices: the role of Ge and III-V materials 88, 419–422.

Schulze, T.F., Korte, L., Rech, B., 2012. Impact of a-Si:H hydrogen depth profiles on passivation properties in a-Si:H/c-Si heterojunctions. Thin Solid Films 520, 4439–4444.

Seba, H.Y., Hadjersi, T., Zebbar, N., Brighet, A., Berouaken, M., Manseri, A., Chabane, L., Kechouane, M., 2020. Alternating current impedance spectroscopic investigation of an a-Si:H/c-Si heterojunction with porous silicon multilayers. Thin Solid Films 699, 137891.

Yousif, B., Abo-Elsoud, M.E.A., Marouf, H., 2019. Triangle grating for enhancement the efficiency in thin film photovoltaic solar cells. Opt. Quantum Electron. 51, 276.

Tables

Table 1. Deposition parameters for layers p-i-n used in solar cells a-Si: H

Deposition parameters	p-i-n		
	p (B_2H_6)	i (H_2/SiH_4)	n (PH_4)
Gas flow ratio (sccm)	2	16	5
Thicknesses (nm)	15	600	25
Band Gap (eV)	2.0	1.68	2.2

Table 2. Deposition parameters for layers p-i_1-i_2-n used in solar cells a-Si: H

Deposition parameters	p-i_1-i_2-n			
	p (B_2H_6)	i_1 (H_2/SiH_4)	i_2 (H_2/SiH_4)	n (PH_4)
Gas flow ratio (sccm)	2	0	36	5
Thicknesses (nm)	15	300	300	25
Band Gap (eV)	2.0	1.90	1.46	2.2

Figures

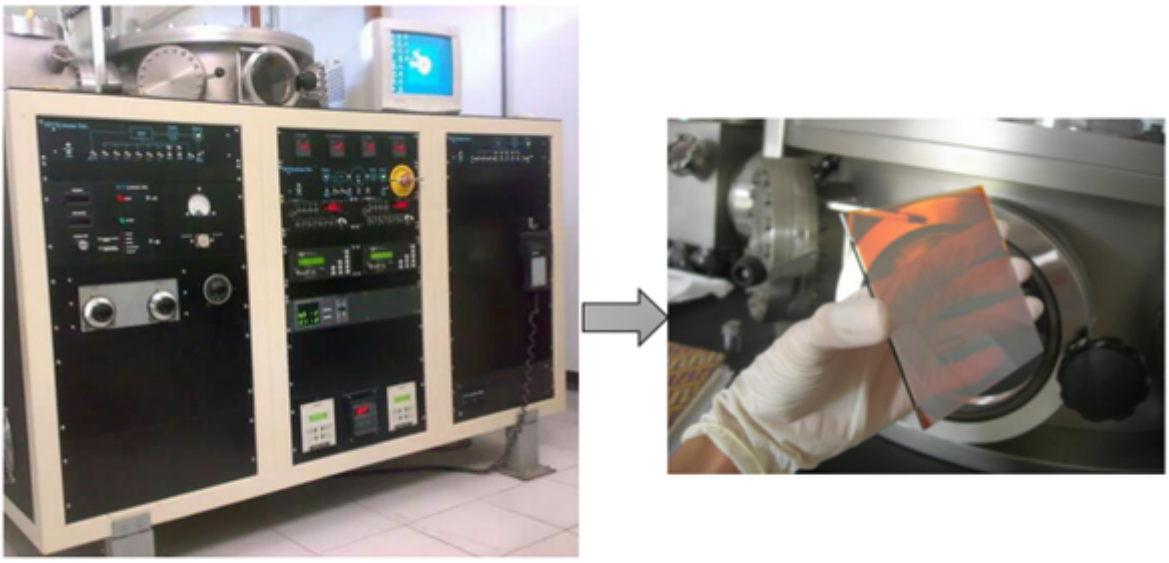

(a) (b)

Figure 1

Sample preparation scheme a-Si:H solar cells. (a) PECVD system with multiple chambers. (b) Samples the amorphous panels (10x10) cm2 are integrated with conductive films.

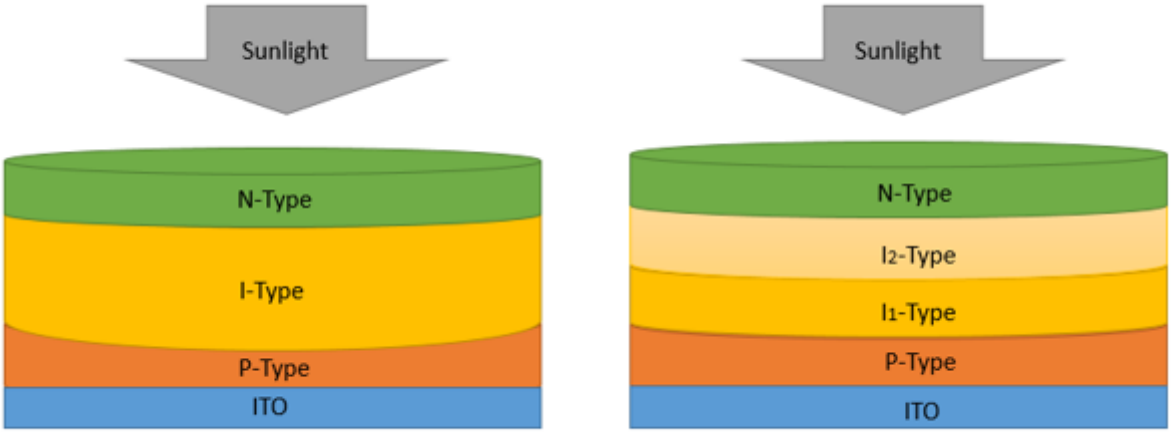

(a) (b)

Figure 2

Schematic of the configuration of a solar cell, showing the textured ITO substrate. (a) p-i-n (b) p-i1-i2-n.

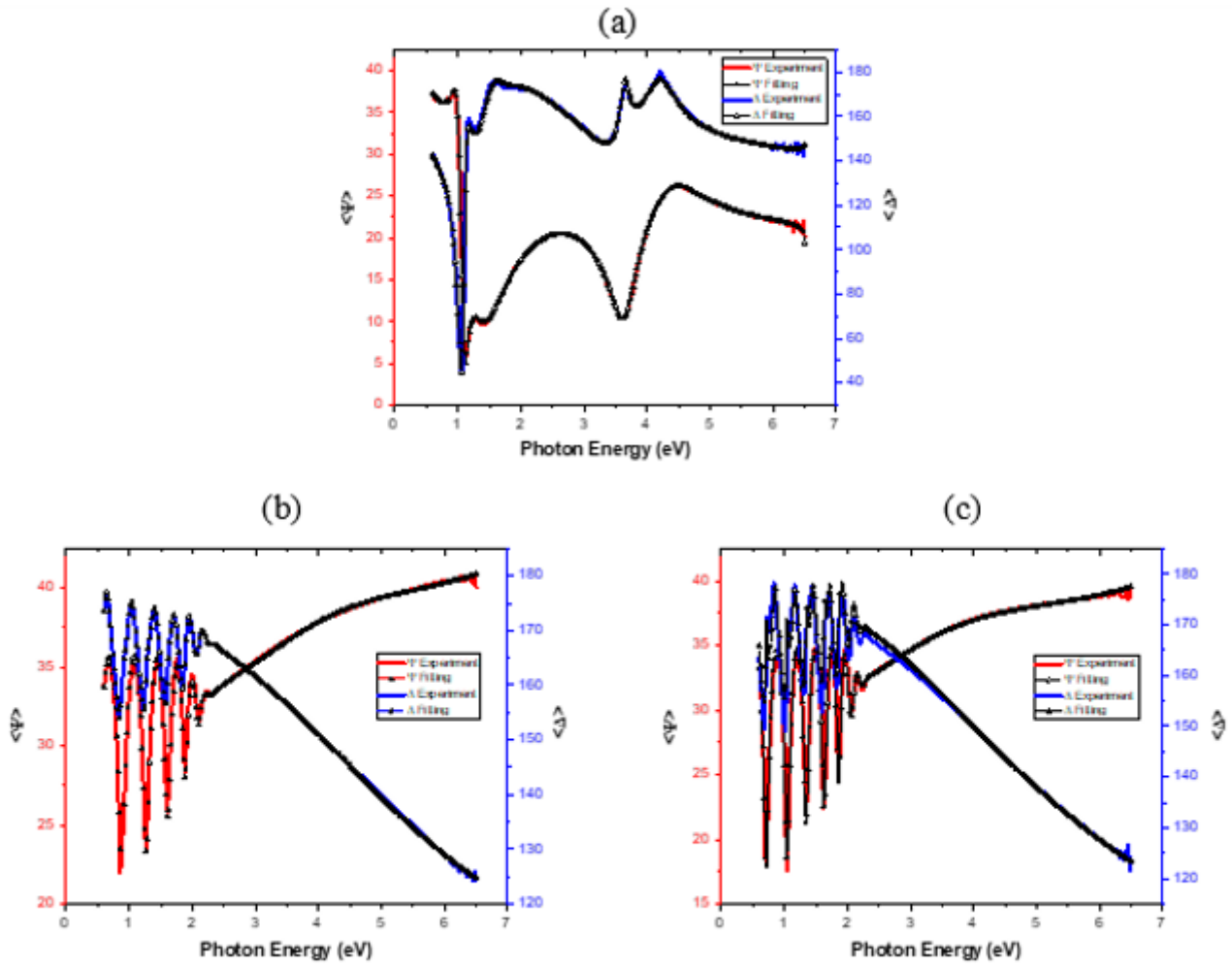

Figure 3

Experimental (solid curves) and fitted (dotted curves) data of Ψ and Δ for ITO (a), (b), p-i-n, and p-i1-i2-n (c) obtained at 70o

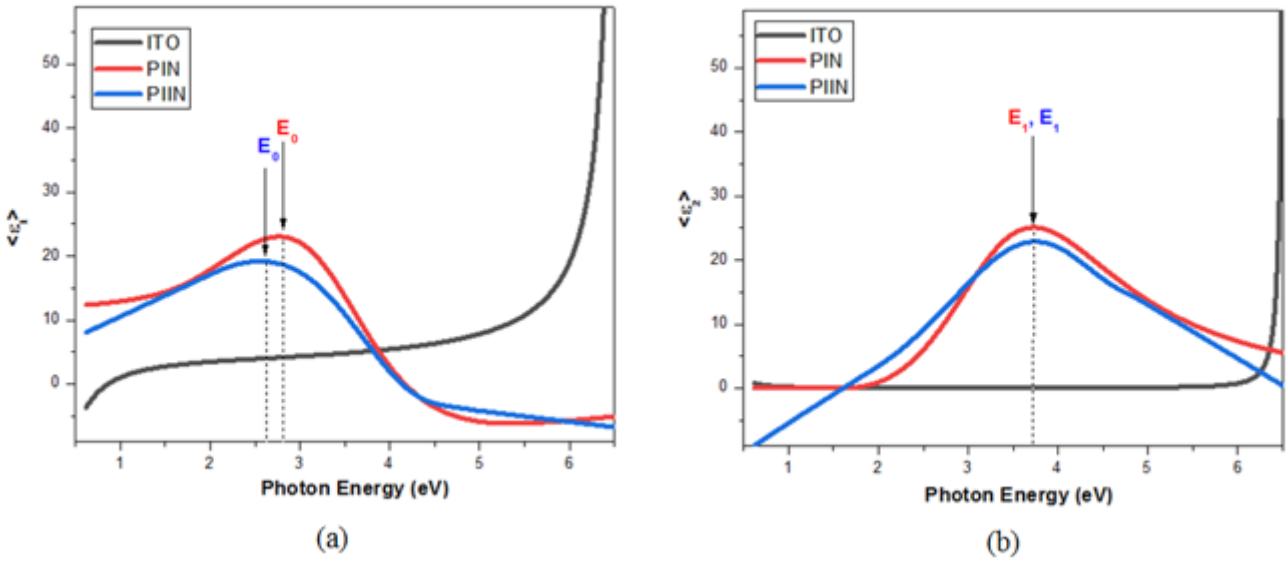

Figure 4

(a) <ε1> of the dielectric function, and (b) imaginary part <ε2> of the dielectric function for ITO, p-i-n and p-i1-i2-n.

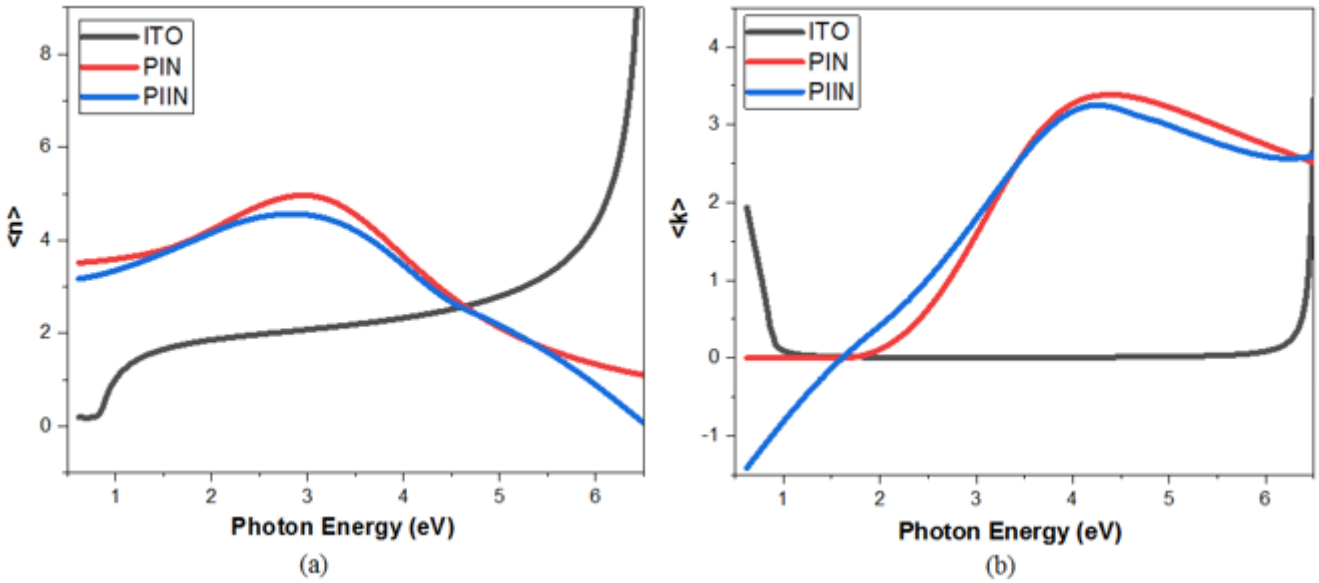

Figure 5

Refractive index (a) <n> and (b) <k> for ITO, p-i-n and p-i1-i2-n.

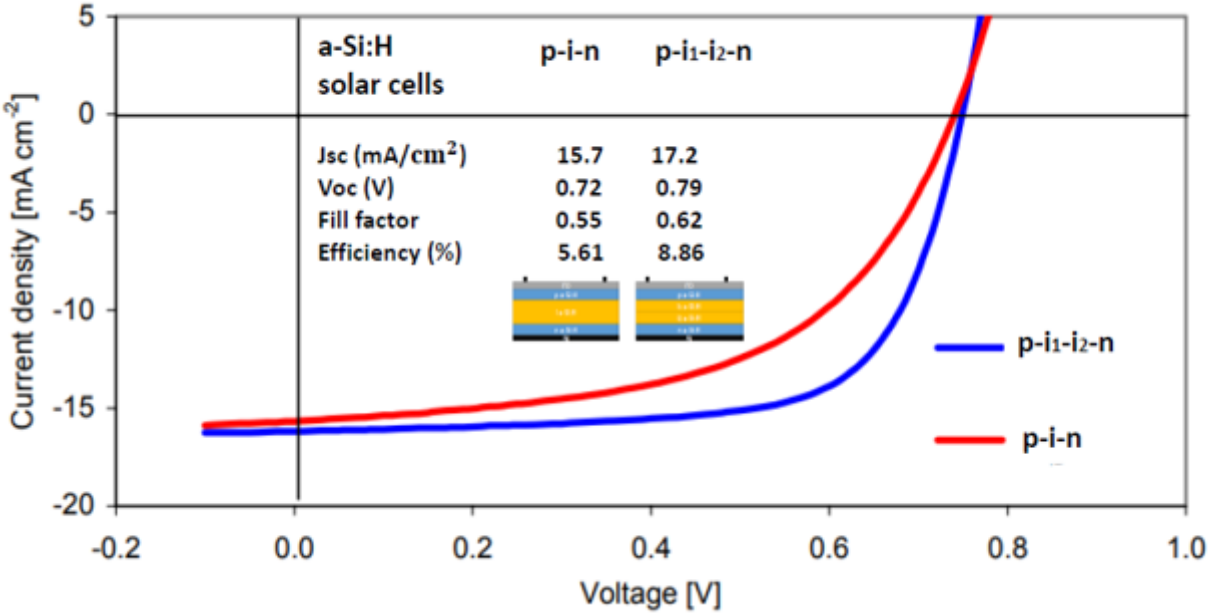

Figure 6

Solar cell efficiency with p-i-n and p-i1-i2-n layers a-Si: H.